

HIGH STEP-UP INTERLEAVED DC-DC CONVERTER WITH PI CONTROLLER FOR RENEWABLE ENERGY APPLICATIONS

Sijinjosephm@gmail.com

1. Muraleedharan MT

Department of Electrical and Electronics
Engineering Government Polytechnic College
,Kalamassery
muraleedharan5149@gmail.com

2. Unnikrishnan P

Department of Electrical and Electronics Engineering
Kerala Government Polytechnic College ,West Hill
unnisrishylam@gmail.com

3. Ajay Kumar EP

Department of Electrical and Electronics
Engineering Sreerama Government Polytechnic
College, Thriprayar
epajay2010@gmail.com

4. Sijin Joseph M

Assistant Engineer
KSEB 220 kv Substation Aluva

5. Basheer K

Department of Electrical and Electronics Engineering
SSM Polytechnic College Tirur
hodelectrical@ssmpoly.ac.in

6. Kamal VV

Department of Electrical and Electronics
Engineering Kerala Government Polytechnic College
,West Hill
vvkamalvv@gmail.com

7. Akhil Ahammed KE

Department of Electrical and Electronics Engineering
kerala Government Polytechnic College ,West Hill
akhilahmedsav@gmail.com

Abstract— This paper proposes a novel high step-up interleaved boost converter suitable for distributed generation using renewable and alternative power sources. The proposed interleaved boost converter not only lengthens the lifetime of the renewable power source by reducing the input-current ripple but also achieves high step-up conversion. In addition, the voltage stress of the main switches is lowered due to the lossless passive-clamp

circuit. Hence, large voltage spikes across the main switches are alleviated and the efficiency is improved. Finally the proposed system offers an excellent dynamic performance for boost the DC voltage that is verified in MATLAB simulink 2017. Experimental setup is also did in scaled down version and its out puts are verified..

I.Introduction

For overcoming energy-shortage and environmental-contamination issues, renewable and alternative power sources that feature cleanliness and sustainability play an important role in the world, and have begun to be employed worldwide for environment protection. The voltage levels of renewable and alternative power sources, such as photovoltaic cells and fuel cells, are generally low. Thus, high-step-up DC-DC converters have been widely utilized in such renewable energy systems in order to boost their voltage levels. The high step-up DC-DC converter can convert low levels of input voltage (typically 40~50V) from renewable sources into high levels of output voltages (typically 380~400V), which are then fed into a DC load or a DC-AC inverter for supplying AC sources with an AC load. Hence, the high-step-up DC-DC converter with high efficiency is essential in such power-conversion systems.

The conventional step-up converters, such as the boost converter and fly back converter, obtain high voltage gain by adopting an extremely high duty cycle or high turns ratio of the coupled inductor. The circuit efficiency of these converters is limited due to the equivalent resistances or from the leakage inductance of windings, and high voltage spikes and stresses occur on the semiconductor devices. Adopting an extremely high duty cycle results in large conduction losses, serious diode reverse-recovery problems, and electromagnetic interference (EMI) issues. Because of the high voltage stresses that occur on the power devices, power switches with low $R_{DS(ON)}$ and power diodes with low reverse-

recovery time cannot be employed in this type of high-step-up converter.

Some existing converters that utilize coupled inductors to achieve high voltage conversion ratio, which recycle the leakage-inductance energy and lower the voltage stresses, have been proposed. Interleaved converter with built-in transformer and interleaved converter with voltage multiplier module or with coupled inductor are another superior solution to obtain high step-up voltage gain and lower input current ripple. The coupled-inductor deals with large DC magnetizing current, so the volume of core is larger and an air gap is required to avoid saturation of core; thus, the cost is higher and the efficiency is lower. On the other hand, the built-in transformer does not deal with large DC magnetizing current, and the voltage gain can be extended by increasing the turn's ratio of the built-in transformer without an air gap; thus, the volume of core is smaller and the coupling coefficient as well as the circuit efficiency is higher. This paper proposes a novel high-step-up interleaved boost converter that not only utilizes the clamp capacitors but also integrates the secondary winding of the built-in transformer; thus, high step-up voltage gain of the presented converter and lower voltage stresses of the power devices are achieved.

The proposed interleaved boost converter with features of high step-up conversion, high circuit efficiency, and low input-current ripple, which can lengthen the life time of the input source, is suitable for distributed generation using renewable and alternative power sources. In addition, windings of the built-in transformer can be designed to extend the step-up gain, and two diodes and two capacitors in

the proposed converter act as an active clamp circuit in order to lower voltage stress on the main switches; thus, low-voltage-rated semiconductor devices (such as power MOSFETs and diodes) can be adopted in the presented converter.

The key characteristics of the proposed converter are listed as follows: (1) Lowering the input-current ripple and reducing the conduction losses results in an increased lifetime of the power sources and makes the presented converter suitable for renewable and alternative energy applications. (2) The converter is capable of achieving high step-up gain easily. (3) By recycling the leakage energy, the voltage stresses of clamp diodes are alleviated and the circuit efficiency is improved. (4) The voltage stresses on the semiconductor components are substantially lower than the output voltage.

Compared with existing converter, the proposed high step-up converter decreases the power switch count and achieves similarly high circuit efficiency without soft-switching function and active clamp circuit. Moreover, the proposed converter has features of cost-effectiveness and relatively low input current ripple in comparison with others.

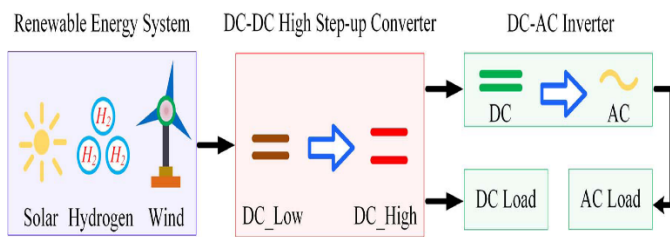
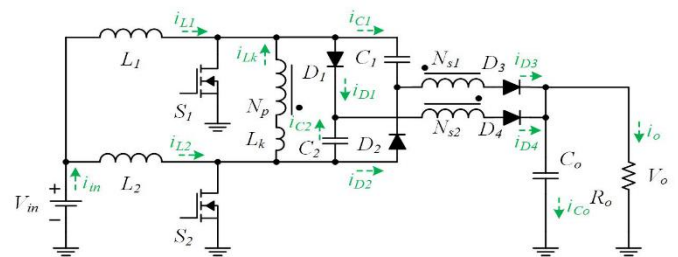


Figure 1.1: Block diagram of distributed generation using renewable power sources

II. INTERLEAVED BOOST CONVERTER

The proposed high-step-up interleaved boost converter is shown in Fig. 4.1, where L_1 and L_2 are the energy storage inductors; S_1 and S_2 denote the power switches; C_1 and C_2 are the clamp capacitors; C_o is the output capacitor; D_1 and D_2 are the clamp diodes, and D_3 and D_4 are the rectified diodes. The built-in transformer consists of a primary winding N_p , a secondary winding N_{s1} , a third winding N_{s2} and a leakage inductor L_k



The gate-driving signals of the two power switches are interleaved with a 180-degree phase shift, and the theoretical waveform of the proposed converter operating in continuous-conduction mode (CCM) is depicted in Fig.4.2.

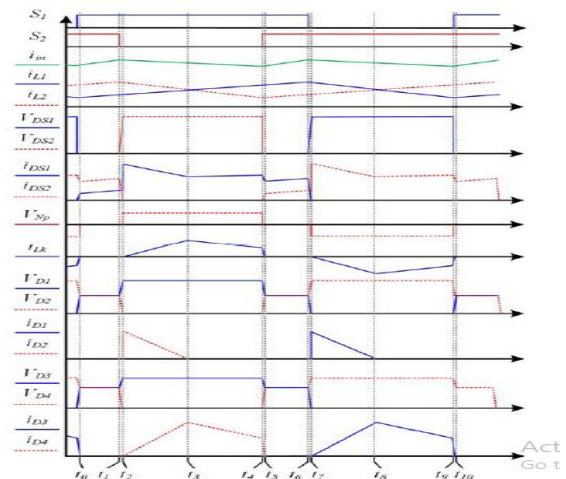


Fig. 4.3 shows the corresponding operational modes of the equivalent circuit. There are 10 main operational modes in one switching period. Due to the completely symmetrical interleaved topology,

operating modes 1 to 5 and 6 to 10 are similar. In order to simplify the analysis of the proposed converter's operating principle, only modes 1 to 5 are analyzed and discussed.

Mode 1 [t_0, t_1]:

At $t=t_0$, both power switches (S_1 and S_2) turn on. All the diodes (D_1, D_2, D_3 , and D_4) are reverse-biased. The path of current flow is shown in Fig. 4(a). Inductors L_1 and L_2 are charged by input voltage V_{in} , and currents through inductors L_1 and L_2 linearly increase

Mode 2 [t_1, t_2]:

At $t=t_1$, power switch S_2 turns off, and its parasitic capacitor is charged by inductor current i_{L2} . The path of current flow is shown in Fig. 4(b).

Mode 3 [t_2, t_3]:

At $t=t_2$, power switch S_2 remains off. The voltages of clamp diode D_2 and rectified diode D_4 decrease; then D_2 and D_4 begin to turn on at $t=t_2$. The path of current flow is shown in Fig. 4(c). The input voltage V_{in} and inductor L_2 provide energy to leakage inductor L_k and primary winding N_p through switch S_1 , and to clamp capacitor C_1 through S_1 and D_2 . The drain-source voltage of power switch S_2 is clamped by capacitor C_1 . The input voltage V_{in} , inductor L_2 , capacitor C_2 and secondary winding N_{s2} provide energy to output capacitor C_o and to load R_o through D_4 .

Mode 4 [t_3, t_4]:

At $t=t_3$, power switch S_2 is still off. The diode current i_{D2} decreases to zero and the clamp capacitor voltage

V_{C1} is equal to the drain-source voltage of power switch S_2 . The path of current flow is shown in Fig. 4(d). The rectified diode current i_{D4} is proportional to leakage-inductor current i_{Lk} .

Mode 5 [t_4, t_5]:

At $t=t_4$, the power switch S_2 turns on. The rectified diode D_4 remains forward-biased because leakage inductor current i_{Lk} still exists. The path of current flow is shown in Fig. 4(e). The leakage inductor current i_{Lk} decreases to zero at $t=t_5$, and rectified diode D_4 begins to be reverse-biased.

In addition, the passive lossless clamp circuit is composed of two capacitors (C_1 and C_2) and two diodes (D_1 and D_2). Referring to *Mode 3* shown in Fig. 4(c), the input voltage V_{in} and inductor L_2 provide energy to the clamp capacitor C_1 through S_1 and D_2 . Thus, the drain-source voltage of power switch S_2 is clamped by capacitor C_1 . Referring to *Mode 8* shown in Fig. 4(h), the input voltage V_{in} and inductor L_1 provide energy to the clamp capacitor C_2 through S_2 and D_1 . Therefore, the drain-source voltage of power switch S_1 is clamped by capacitor C_2 .

4.2. VOLTAGE STRESS AND VOLTAGE STRAIN

The voltage on clamp capacitors C_1 and C_2 can be expressed as

$$V_{C1} = V_{C1} = \frac{1}{1-D} V_{in}$$

The voltage on output capacitor C_0 can be derived

from

$$V_{C0} = \frac{2+n}{1-D} V_{in}$$

The output voltage V_0 is given by

$$V_0 = V_{C0} = \frac{2+n}{1-D} V_{in}$$

In addition, the voltage gain of the proposed converter is described as

$$\frac{V_0}{V_{in}} = \frac{2+n}{1-D}$$

The voltage stresses on power switches S_1 and S_2 are clamped, and are derived from

$$V_{DS1} = V_{DS2} = \frac{1}{1-D} V_{in}$$

The voltage stress on diodes D_1 , D_2 , D_3 and D_4 are respectively given by

$$V_{D1} = V_{D2} = \frac{2}{1-D} V_{in}$$

And

$$V_{D3} = V_{D4} = V_0 = \frac{2+n}{1-D} V_{in}$$

2.3 DESIGN CONSIDERATIONS

In the proposed high step-up interleaved boost converter, the input current I_{in} and the ripple current Δi_L of the inductor are represented by

$$I_{in} = \frac{2+n}{1-D} I_0 = \left(\frac{2+n}{1-D}\right)^2 \frac{V_{in}}{R_0}$$

And

$$\Delta I_L = \frac{V_{in} \cdot D}{f_s \cdot L_1} = \frac{V_{in} \cdot D}{f_s \cdot L_2}$$

The relationship between input current I_{in} and the ripple current Δi_L of the inductor in boundary-conduction mode (BCM) is given by

$$\frac{I_{in}}{2} = \frac{\Delta I_L}{2}$$

Substituting all the equations, the boundary condition for the normalized inductor time constant, which is represented by τ_{LB} , is

expressed by

$$\tau_{LB} = \frac{L_1}{R_0} \cdot f_s = \frac{L_2}{R_0} \cdot f_s = \frac{D \cdot (1-D)^2}{(2+n)^2}$$

Fig.4.4 shows the relationship between the boundary condition for the normalized inductor time constant τ_{LB} and duty cycle D under a turns-ratio n of 1 according to equation, and this figure is a design guideline for selecting appropriate inductors L_1 and L_2 of the presented converter.

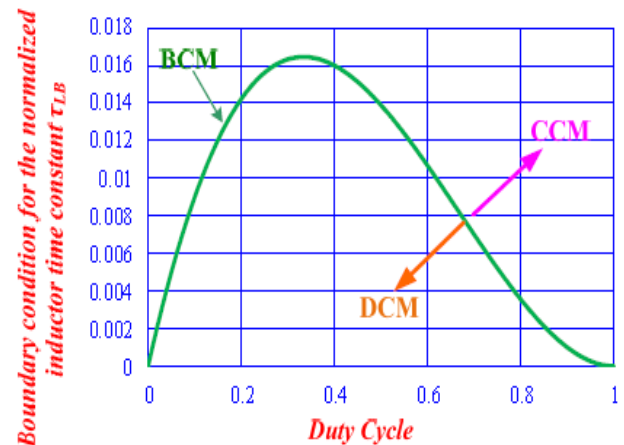


Fig.4.4. The relationship between boundary condition for the normalized inductor time constant τ_{LB} and duty cycle

III. SIMULATION INTERLEAVED BOOST CONVERTER

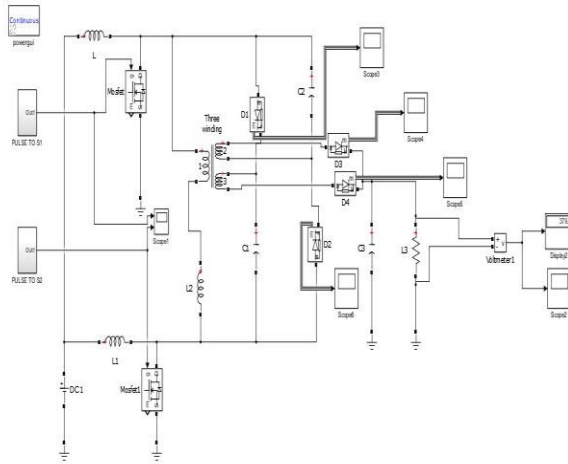


Fig.3.1. Simulation model of the interleaved boost converter

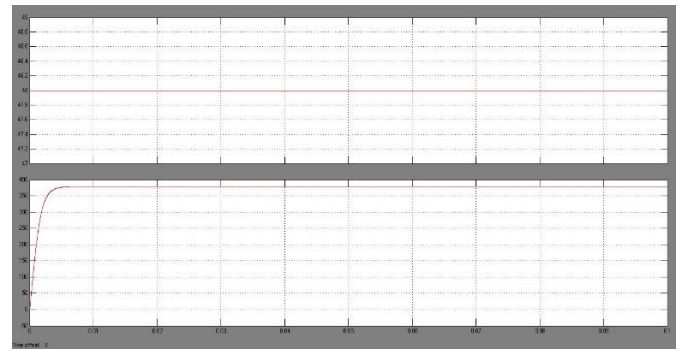


Fig 3.3 Input and output voltage of interleaved boost converter

IV Hardware implementation and results

7.1. HARDWARE DESCRIPTIONS

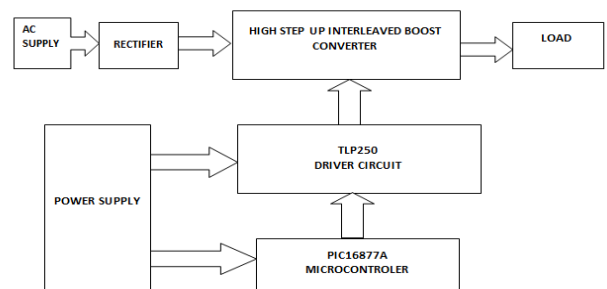


Fig 4.1 Block Diagram of Experimental Set up

3.2. VOLTAGE STRESS COMPARISON

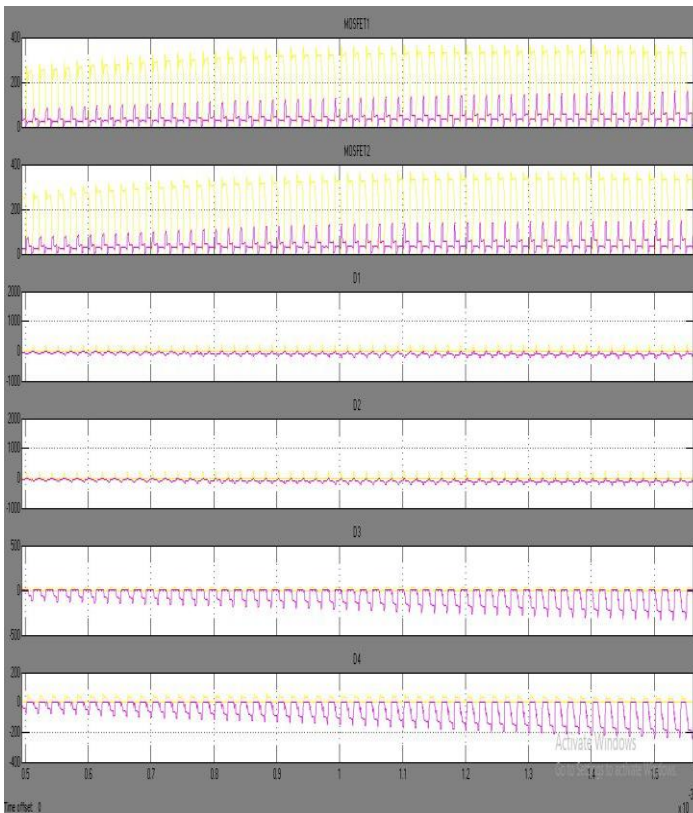


Fig 3.2. Voltage stress comparison of the proposed interleaved boost converter



Fig. 4.2 Hardware

converter, this methodology can be used for energy harvesting.

VI Reference

1. J. T. Bialasiewicz, "Renewable energy systems with photovoltaic power generators: Operation and modeling," *IEEE Trans. Ind. Electron.*, vol. 55, no. 7, pp. 2752–2758, Jul. 2008
2. B. Yang, W. Li, Y. Zhao, and X. He, "Design and analysis of a grid-connected photovoltaic power system," *IEEE Trans. Power Electron.*, vol. 25, no. 4, pp. 992–1000, Apr. 2010
3. T. Kefalas, and A. Kladas, "Analysis of transformers working under heavily saturated conditions in grid-connected renewable energy systems," *IEEE Trans. Ind. Electron.*, vol. 59, no. 5, pp. 2342–2350, May. 2012
4. R. J. Wai, W. H. Wang, and C. Y. Lin, "High-performance stand-alone photovoltaic generation system," *IEEE Trans. Ind. Electron.*, vol. 55, no. 1, pp. 240–250, Jan. 2008.
5. R. J. Wai, and W. H. Wang, "Grid-connected photovoltaic generation system," *IEEE Trans. Circuits Syst. I, Reg. Papers*, vol. 55, no. 3, pp. 953–964, Apr. 2008
6. L. Gao, R. A. Dougal, S. Liu, and A. P. Iotova, "Parallel-connected solar PV system to address partial and rapidly fluctuating shadow conditions," *IEEE Trans. Ind. Electron.*, vol. 56, no. 5, pp. 1548–1556, May 2009
7. K. C. Tseng, C. C. Huang, and W. Y. Shih, "A high step-up converter with a voltage multiplier module for a photovoltaic system," *IEEE Trans. Power Electron.*, vol. 28, no. 6, pp. 3047–3057, Jun. 2013
8. S. K. Changchien, T. J. Liang, J. F. Chen, and L. S. Yang, "Novel high step-up DC-DC converter for fuel cell energy conversion system," *IEEE Trans. Ind. Electron.*, vol. 57, no. 6, pp. 2007–2017, Jun. 2010
9. K. C. Tseng, J. Z. Chen, J. T. Lin, C. C. Huang, and T. H. Yen, "High step-up interleaved forward-flyback boost converter with three-winding coupled inductors" *IEEE Trans. Power Electron.*, vol. 30, no. 9, pp. 4696–4703, Sep. 2015